



Rheological properties of microfibrillated cellulose and hydroxypropyl methylcellulose blends in ethanol/water solvent systems

Egon Petersohn Junior · Angelo Cezar Lucizani · Victor Veríssimo · Cassiano Pires · Alan Sulato de Andrade · Mailson de Matos · Gisele Perissutti · Washington Luiz Esteves Magalhaes · Rilton Alves de Freitas

Received: 7 February 2024 / Accepted: 21 July 2024 / Published online: 29 July 2024
© The Author(s), under exclusive licence to Springer Nature B.V. 2024

Abstract Microfibrillated cellulose (MFC) and hydroxypropyl methylcellulose (HPMC) were employed as gelling agents in hydroalcoholic solutions. However, a limited number of studies have explored the interactions between MFC and cellulose derivatives in organic solvents. Most of these studies have primarily focused on either the interactions between MFC and polymers in aqueous solutions. To

investigate their collaborative effect, phase diagrams were constructed by varying the concentration of the constituent elements, confirming phase separation, and identifying liquid-like and gel-like properties through oscillatory rheological measurements. Oscillatory amplitude, frequency, oscillatory swing temperature and viscosity were performed. Additionally, aerogels were fabricated with and without ethanol for microscopic analysis. It was demonstrated that ethanol significantly influences the rheological characteristics of MFC and MFC+HPMC dispersions, resulting in an increase in the elastic modulus (G'), decreased thixotropic behavior, and increased stability. Tests were also conducted with urea, a strongly chaotropic agent, providing evidence of the types of interactions governing the systems, and demonstrating that intermolecular hydrogen bond interactions play a predominant role.

Supplementary Information The online version contains supplementary material available at <https://doi.org/10.1007/s10570-024-06085-3>.

E. P. Junior · A. C. Lucizani · V. Veríssimo · W. L. E. Magalhaes
Integrated Program in Engineering and Materials Science,
Federal University of Paraná, Polytechnic Center,
Curitiba 81531-990, Brazil

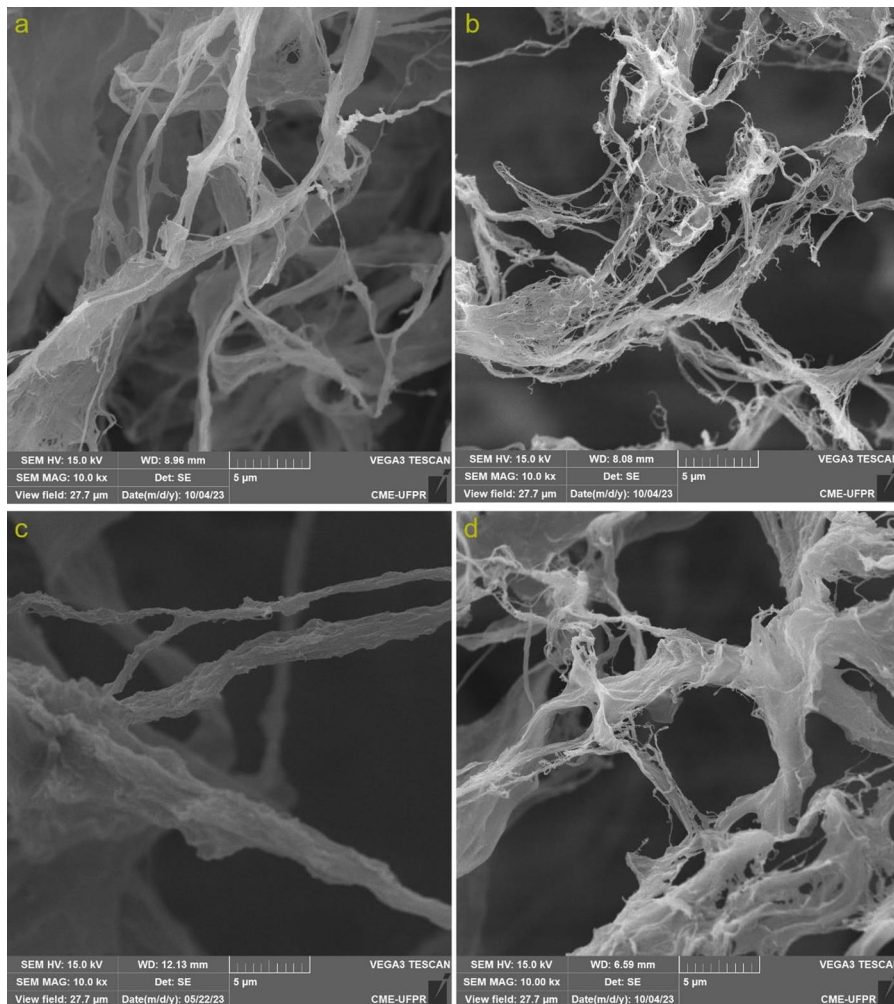
C. Pires · R. A. de Freitas (✉)
Biopol, Pharmacy Department, Federal University
of Paraná, Curitiba, PR 80210-170, Brazil
e-mail: rilton@ufpr.br

A. S. de Andrade
Department of Forest Engineering and Technology,
Federal University of Paraná, Curitiba, PR 80210-170,
Brazil

M. de Matos
SENAI Institute of Innovation in Electrochemistry,
Curitiba, PR, Brazil

G. Perissutti · W. L. E. Magalhaes
Embrapa Florestas, Estrada da Ribeira, Km 111,
Colombo 83411-000, Brazil

Graphical Abstract



Keywords Microfibrillated cellulose · Hydroxypropyl methylcellulose · Hydroalcoholic solutions · Rheology

Introduction

According to IUPAC (2006), gel is a non-fluid colloidal network or polymer network that is expanded throughout its whole volume by a fluid. These networks limit the solvent flow and can be formed from various materials and solvents, each imparting specific characteristics to the resulting gel. Such gels find application across diverse fields such as food,

biology, medicine, and pharmaceuticals (Nath et al. 2023; Xu 2009; Rathod and Mehta 2015). Particularly noteworthy are alcogels, formed from alcohol and gelling agents, which have garnered significant interest across industries (Cassanelli et al. 2017).

Alcohol gels, a type of organogels, offer versatile properties such as the ability to dissolve both hydrophobic and hydrophilic compounds and act as antisolvents (Onori and Santucci 1996; Joye and McClements 2013). These characteristics enable their application including disinfection, edible products, anti-freezing agents, and bioactive drug delivery systems (Gold et al. 2023; Villa and Russo 2021; Jian et al. 2021; Zhang et al. 2022).

To produce alcohols, a range of gelling agents can be employed, including cellulose derivatives, which are notable for their renewable, biodegradable, and abundant nature (Nechyporchuk et al. 2016; da Silva et al. 2018). Among these derivatives, microfibrillated cellulose (MFC) has attracted significant attention due to its nanometric scale and potential applications (Klemm et al. 2011). Studies have elucidated very interesting rheological properties of MFC, modulated by several factors such as concentration, pH, salts, organic solvents, cellulose derivatives, and carbohydrates (Pääkko et al. 2007; Rezayati-Charani et al. 2013; Costa et al. 2019; Kokol 2022; Lameirinhas et al. 2023).

The use of cellulose derivatives, such as Hydroxypropyl Methylcellulose (HPMC), in modulating the rheological behavior of nanocellulosic materials has received significant interest (Echeverria et al. 2016; Kokol 2022; Sorvari et al. 2014). HPMC, widely employed in pharmaceutical, food, and dietary supplement industries, exhibits versatile physicochemical attributes influenced by factors such as molar mass, degree of substitution, and solvent composition (Burdock 2007; Mašková et al. 2020).

However, despite existing research on MFC and cellulose derivatives in water, a gap remains in understanding the behavior of MFC with cellulose derivatives dispersed in organic solvents. This gap presents an opportunity for investigation, offering potential insights for developing new materials and products, including applications in pharmaceuticals, aerogels, scaffolds, and coatings. In this context, our study aims to evaluate the rheological behavior of MFC in conjunction with ethanol and HPMC, providing comprehensive insights into their interactions and potential applications. We present three meticulously developed phase diagrams, investigating the effects of ethanol concentrations on MFC, HPMC, and their combination, utilizing oscillatory rheology and scanning electron microscopy for comprehensive analysis.

Experimental

Materials

The commercial MFC from bleached eucalyptus pulp (Klabin S.A.—Paraná/Brazil) was purchased in gel form (3.99 w/w%) and used as the raw materials.

The cellulases mix Maximize® 2570 was purchased from Buckman (Memphis, TN, USA). For the ammonium acetate buffer solution was used ammonium acetate from Sigma-Aldrich (USA) and acetic acid from Alphatec® (Brazil). Moricell F (HPMC) was obtained from MC Química (São Paulo, Brazil). The mass average molar mass (M_w) was $5.7 \times 10^5 \text{ g mol}^{-1}$; number average molar mass (M_n) of $4.9 \times 10^5 \text{ g mol}^{-1}$ and dispersity (\mathcal{D}) of 1.2. Wet and ash content was determined as 1.3 and 0.0, respectively. Substitution degree (DS) was calculated for methyl (DS_M) and hydroxypropyl (DS_P) by $^1\text{H-NMR}$ and were 0.35 and 0.12, respectively. Ethanol 99.5 w/w% was obtained from Sigma-Aldrich (USA).

Methods

Enzymatic/Mechanical post-treatment

To enhance the properties of MFC as a rheological modifier, samples underwent to enzymatic/mechanical post-treatment, employing the enzyme mix Maximize 2570. This post-treatment aimed to achieve finer defibrillation of the MFC, leading to increased viscosity of the gel suspension. The process involved enzymatic assistance to facilitate mechanical processing with a reduced number of passes. Preliminary data, yet unpublished, indicates that the enzyme treatment resulted in MFC with higher elastic and viscous moduli, as well as viscosity, requiring only half the passes compared to treatments without enzymes under similar conditions. Additionally, a decrease in the intrinsic viscosity of the MFC was observed, along with an increase in crystallinity.

Initially, the MFC concentration was adjusted to 1 w/w% of solids in a 10 mM ammonium acetate buffer at pH 5.5. Subsequently, 1 mg/g of enzyme was added relative to the dry mass of MFC, and the mixture was incubated at 25 °C in a water batch under constant stirring for 49 min. The treated MFC was then processed using a Super Masscolloider Masuko Sangyo mill (Masuko, Japan) operating at 1500 rpm and a flow rate of 0.5 L/min for 10 passes. Following processing, the MFC was heated to 80 °C for 10 min to deactivate the enzymes.

In unpublished data, enzymatic treatment was found to decrease polymerization degree and increase crystallinity, as evidenced by intrinsic

viscosity and XRD analysis. Despite this, the enzymatic cocktail Maximyze® 2570 does not convert cellulose into sugars, making it suitable for MFC production to prevent losses in cellulose depolymerization. Furthermore, enzymatic treatment modifies suspension rheology, enhancing elastic and viscous moduli, apparent viscosity, and significantly reducing the number of passes needed to achieve optimal levels. This reduction in processing steps is essential for the economic feasibility of MFC production, resulting in energy and time savings.

Phase diagram

Three phase diagrams were obtained: a pseudo-ternary diagram comprising MFC, HPMC, ethanol, and water, with MFC and HPMC concentrations ranging from 0.1 to 1.0% and 0.04 to 0.4%, respectively, and ethanol concentrations varying from 0.0 to 90%; and two ternary diagrams. One ternary diagram included MFC, ethanol, and water, with MFC concentrations ranging from 0.1 to 1.0% and ethanol concentrations varying from 0.0 to 90%. The other ternary diagram comprised HPMC, ethanol, and water, with HPMC concentrations ranging from 0.2 to 1.6% and ethanol concentrations varying from 0.0 to 90%.

The sample preparation procedure for the pseudo-ternary phase diagram involved adding HPMC to the ethanol/water mixture while stirring magnetically until complete solubilization (colloidal dispersion). Subsequently, MFC was added, and the samples were further mixed by magnetic stirring until complete macroscopically homogenization was achieved. For the ternary diagrams, either MFC or HPMC was introduced into the ethanol/water mixture under magnetic stirring and stirred until the sample was macroscopical homogenization. The suspensions' behavior was evaluated visually and through frequency sweep rheological tests after 24 h.

To investigate the participation of intermolecular hydrogen bonds in the network formation of MFC and MFC + HPMC gels, dispersions were prepared with 6 M urea, a known hydrogen bond disrupting agent, which can, collaterally, weaken hydrophobic interactions. For this, urea was solubilized under magnetic stirring followed by the addition of other polymers according to the procedure described above.

Rheological characterization

Dynamic oscillatory measurements were performed using a Discovery Hybrid HR-10 rheometer (TA Instruments., New Castle, DE, USA), with a cone-plate configuration (40 mm diameter, 2° cone angle and truncation gap of 0.101 mm), coupled to a Peltier system. First, amplitude sweeps were performed in the range of 0.001 to 500 Pa at a constant frequency of 10 Hz, to determine the linear viscoelastic region (LVR), which was used for the other tests. Then, frequency sweeps were performed on the LVR, where the storage (G') and loss (G'') modulus were recorded, as well as the loss tangent ($\tan \delta$) as a function of frequency between 0.01 and 10 Hz.

Flow sweeps experiments were performed under steady state conditions for data reproducibility and to remove the effect of thixotropy, determined experimentally and using a shear rate ramp from 1 to 100 s^{-1} and followed by another ramp from 100 to 1 s^{-1} , with 300 s for each ramp. Operating conditions were 25 °C, equilibrium time of 60 s and 5 points per decade.

The oscillatory swing temperature test was performed between 5 and 50 °C with a heating rate of 10 °C/min, at a constant frequency of 1 Hz and a constant stress of on the LVR. To avoid solvent evaporation, solvent trap was used. Then, the temperature ramp was performed in cooling mode from 50 to 5 °C under the same conditions. These temperature sweeps were repeated three times to identify any sign of sample instability.

Zeta potential

To evaluate the impact of ethanol and HPMC on the Zeta potential of MFC, samples of MFC 0.1 w/w%, HPMC 0.1 wt% and MFC 0.1 wt% + HPMC 0.04 wt% were prepared in different concentrations of ethanol. The zeta potential was determined using Particle Metrix—Stabino® equipment and model PMX 400, with measurements every 5 s for a period of 5 min.

Results and discussion

Phase diagram

Figure 1 presents phase diagrams illustrating dispersions of MFC (Fig. 1a), HPMC (Fig. 1b), and

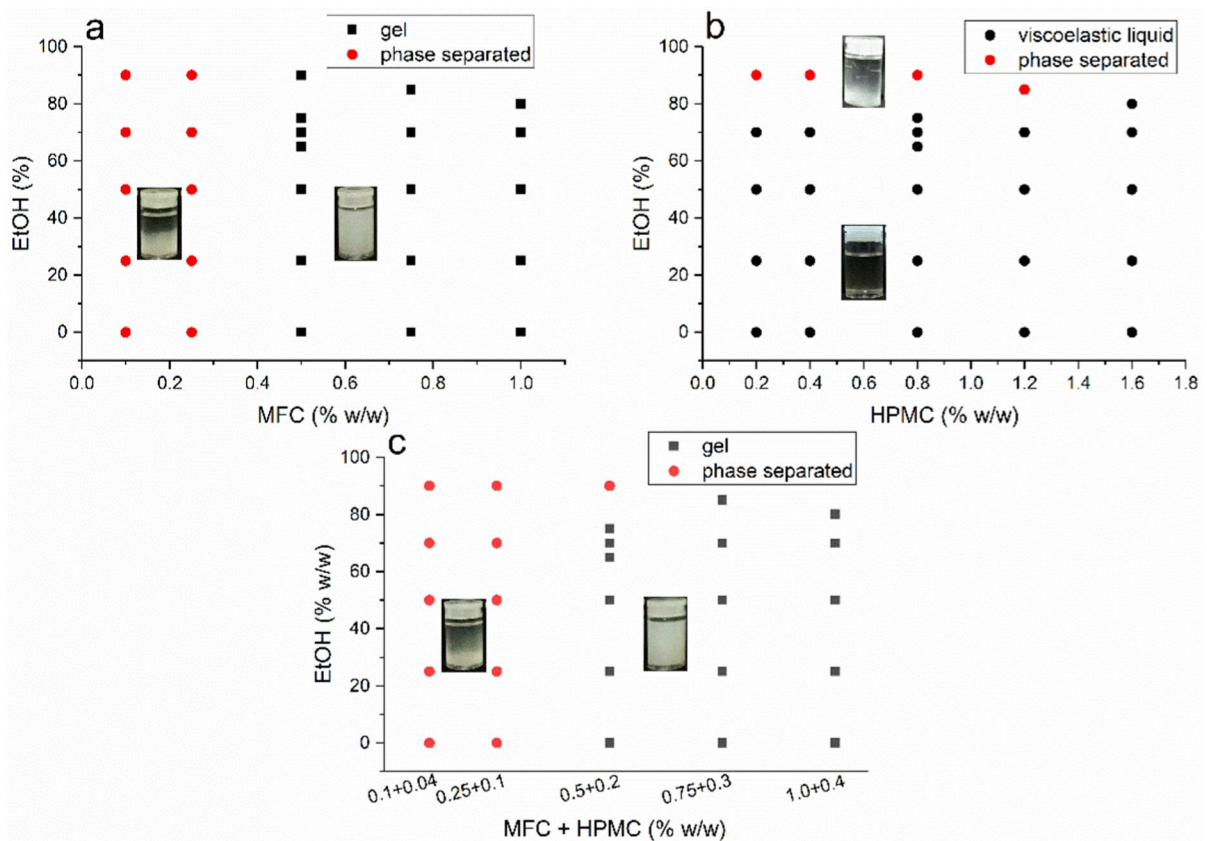


Fig. 1 Phase diagram of polymers-ethanol/water mixtures. The gel state was defined by frequency sweep when the sample exhibit $G' > G''$. **a** Microfibrillated cellulose-ethanol/water (MFC-EtOH). **b** (Hydroxypropyl)methyl cellulose-ethanol/water (HPMC-EtOH). **c** Microfibrillated cellulose/hydroxypropylmethylcellulose -ethanol/water (MFC + HPMC-EtOH), MFC:HPMC ratio 1:0.4. Black square: gel (a–c) and viscoelastic liquid (b). Red circle: phase separated

MFC+HPMC (Fig. 1c) in various ethanol/water concentrations. Macroscopic observations of gel or liquid properties were made by tilting the tube and further confirmed by oscillatory rheology, where an ideal gel elastic, the G' value is anticipated to remain frequency-independent, with G' exceeding G'' (Peng et al. 2018; Tzoumaki et al. 2013).

In MFC dispersions (Fig. 1a), phase separation occurs when MFC concentrations fall below 0.25 w/w%, irrespective of ethanol concentration. This phenomenon is likely linked to the gel point concentration, representing the critical consistency at which a continuous network of fibers in suspensions forms, leading to a self-supporting network (Gourlay et al. 2018; Raj et al. 2016). MFC concentrations surpassing 0.5 w/w% displayed gel-like behavior, suggesting that the solids content predominantly governs

network formation, with minimal impact from the ethanol/water mixture.

water (HPMC-EtOH). **c** Microfibrillated cellulose/hydroxypropylmethylcellulose -ethanol/water (MFC + HPMC-EtOH), MFC:HPMC ratio 1:0.4. Black square: gel (a–c) and viscoelastic liquid (b). Red circle: phase separated

network formation, with minimal impact from the ethanol/water mixture.

In Fig. 1b, viscoelastic liquid-like behavior is observed at ethanol concentrations below 80 w/w%, regardless of polymer concentration. This behavior can be attributed to the hydroxypropyl groups of HPMC, which disrupt intermolecular hydrogen bonds (Wang et al. 2018). Conversely, phase separation occurs at ethanol concentrations exceeding 85 w/w%. Ethanol is known to act as an anti-solvent, leading to polymer precipitation at high concentrations (Tian et al. 2022). Perinelli et al. (2021), studying alcohol-based hand sanitizers employing cellulose derivatives, propose that at elevated ethanol concentrations, interactions between polymeric chains may intensify, reducing the hydration shell and promoting polymer aggregation, ultimately resulting in precipitation.

The behavior of MFC+HPMC mixtures across varying ethanol concentrations is presented in Fig. 1c. Similar to MFC dispersions, phase separation occurs at polymer+fiber concentrations below 0.35 w/w% (MFC 0.25 w/w%/HPMC 0.10% w/w%), and gel-like behavior is observed above 0.70 w/w% (MFC 0.50 w/w%/HPMC 0.20 w/w%), with one exception at the point MFC +HPMC 0.70 w/w%/EtOH 90 w/w%.

Hypothetically, it is probable that HPMC becomes adsorbed onto MFC chains, where primary interactions occur within ethanol/water solutions. An indication of HPMC adsorption on MFC fibrils is the observed reduction in zeta potential (Mosse et al. 2012), a point we will discuss briefly in this manuscript.

Butchosa and Zhou (2014) demonstrated the adsorption of CMC onto cellulose nanofibers through conductometric titration. Here, we supposed that at higher ethanol concentrations, interactions among HPMC chains intensify, leading to polymer aggregation and subsequent co-precipitation of HPMC with MFC when MFC concentrations are low. The occurrence of phase separation at low concentrations likely correlates with the gel point concentration, as discussed earlier. At higher polymer concentrations, the gel-like behavior is probably governed by the elevated MFC concentrations, which establish a robust network structure.

Rheological properties

Frequency sweep

Frequency sweep measurements are conducted to assess the structural integrity and mechanical strength of materials (Yuan et al. 2018; Zhou et al. 2020). Figure 2 and SI-1 (Supplementary Information 1) present frequency sweeps for the MFC, HPMC, and MFC+HPMC dispersions across various ethanol concentrations and polymer concentrations. The MFC dispersions (Fig. 2a) exhibit $G' > G''$ across the entire frequency range, with both moduli being nearly frequency-independent, indicating gel like system (Jia et al. 2015).

In HPMC dispersions (Fig. 2b), G'' surpasses G' , and both moduli exhibit frequency dependence, escalating as the frequency rises, indicative of a liquid-like viscoelastic behavior (Baby 2019).

MFC+HPMC dispersions exhibit a hybrid behavior, reflecting the influence of both cellulose nanofiber and polymer. Like MFC dispersions, MFC+HPMC systems (Fig. 2c) display $G' > G''$, characteristic of solid-like behavior at total concentrations $\geq 0.7\%$. However, unlike MFC dispersions, both moduli of MFC+HPMC are frequency-dependent, escalating with increasing frequency, likely attributable to HPMC. This behavior indicates the formation of weak gels (Naeli et al. 2020).

The differences between MFC and MFC+HPMC dispersions are clearly delineated in Fig. SI-1. MFC+HPMC moduli are notably lower and more frequency-dependent (Adeyeye et al. 2002). The decline in $\tan \delta$ at low frequencies, observed to MFC+HPMC, correspond to an increase in terminal relaxation time, indicative of quasi-permanent or permanent network presence. Additionally, we suppose the reduction in modulus resulting from HPMC presence suggests weakened fiber interactions or fewer contact points between them, indicating HPMC's role in dispersing the MFC suspension (Sorvari et al. 2014).

Nanocellulosic materials such as MFC exhibit polar characteristics that interact with hydrophilic groups along HPMC molecule backbones (Bilbao-Sáinz et al. 2010). The shared backbone structures of both fibers and polymers suggest that adsorption might align HPMC chains with MFC chains, potentially keeping cellulose fibrils separated and reducing frictional forces (Hubbe et al. 2017). This phenomenon mirrors the behaviour observed in other polymers like CMC, HEC, and xanthan gum (Kokol 2022; Sorvari et al. 2014).

Figure 3 illustrates the impact of ethanol concentration on G' , G'' , and $\tan \delta$ in MFC dispersions, HPMC, and MFC+HPMC mixtures.

Notably G' increases with ethanol concentration, as evidenced in Figs. 3a and 3c, with $\tan \delta$ exhibiting a continuous decline from 0.29 to 0.15 for MFC and MFC+HPMC. This decline and the concurrent rise in G' indicate a progressive increase in system stiffness. Similar observations were made by da Silva et al. (2018), suggesting a connected fibril network formation or loss of mobility due to increased excluded volume.

Hypothetically, the progressive stiffening of MFC dispersions can partly be attributed to zeta potential modulus decay with increasing ethanol concentration,

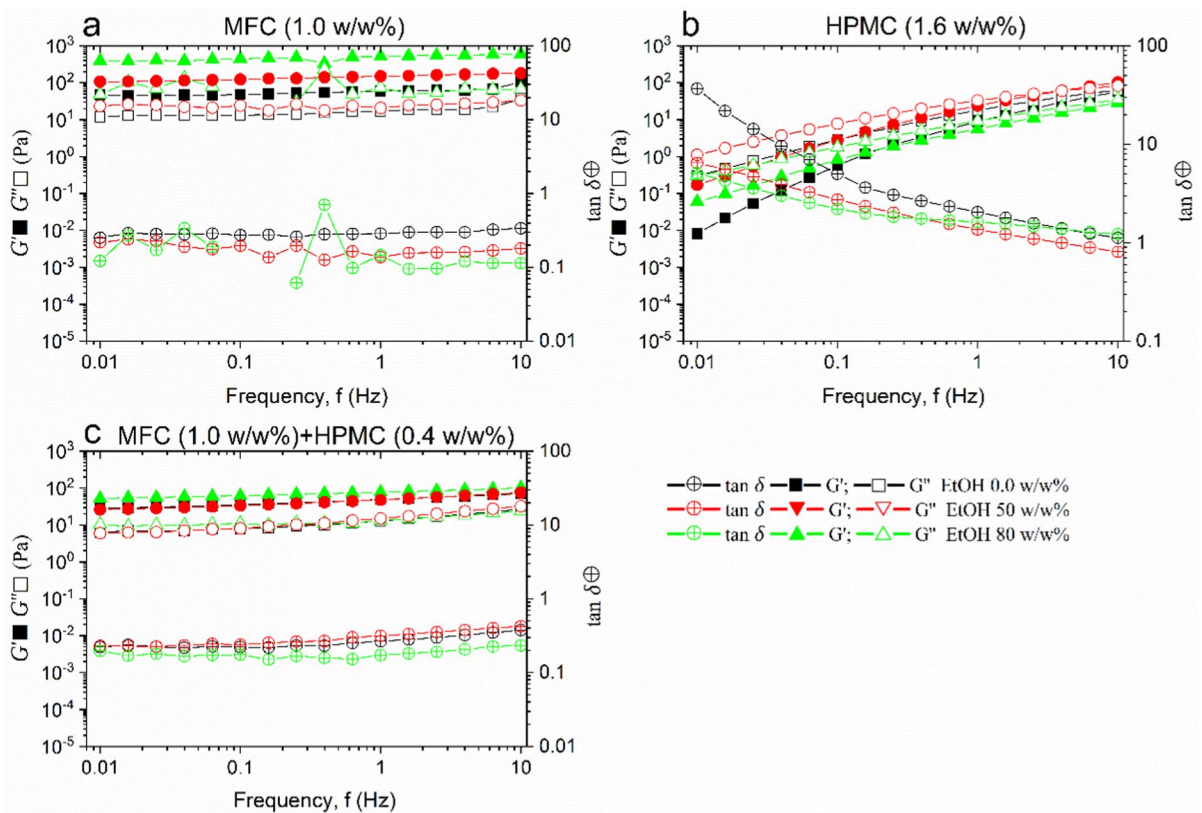


Fig. 2 Oscillatory frequency sweep, performed in a linear viscoelastic regime at constant temperature 25 °C. Figures **a–c** storage modulus G' (solid symbols), loss modulus G'' (open symbols) and $\tan \delta$ (circle with + center). 0.0 w/w % ethanol: black symbols. 50 w/w % ethanol: red symbols. 80 w/w % ethanol: green symbols. **a** Storage and loss modulus for 1 w/w%

MFC dispersions in different ethanol concentrations; **b** storage modulus and loss modulus for 1.6 w/w% HPMC in different ethanol concentrations. HPMC **d** storage modulus and loss modulus for 1 w/w% MFC + 0.4 w/w% HPMC in different ethanol concentrations

a result of ethanol/water interaction (Gözcü et al. 2023). Additionally, microdomain formation in water/alcohol mixtures, resulting from water and alcohol molecule self-association, may lead to non-homogeneous groupings (Dixit et al. 2002; Wakisaka et al. 2001). These microdomains could segregate MFC, concentrating in decreasing water domains as alcohol content rises (da Silva et al. 2018). Also, cellulose's type I combined with ethanol, could enhance MFC hydrophobic interactions (Medronho et al. 2012; Morel et al. 2020; Vorontsova et al. 2015). However, further studies are needed to comprehensively understand all mechanisms involved in MFC and alcohol/water system interactions.

It's plausible that HPMC becomes adsorbed onto cellulose microfibrils, possibly enveloping them and hindering direct fiber-to-fiber contact. This could

weaken interactions between fibers or reduce the number of contacts between them. In an alcoholic medium, as observed, the hydration layer diminishes, enhancing inter/intrachain interaction of HPMC. However, at higher ethanol concentrations, interaction between HPMC chains might intensify, further reducing the hydration layer and prompting polymer aggregation, ultimately leading to precipitation. In the case of MFC + HPMC mixtures, it's conceivable that at high ethanol concentrations, partial desorption of HPMC from the surface of MFC fibrils occurs, partially restoring contact between MFC fibrils. This elucidates the increase in G' and the decrease in $\tan \delta$ observed when the ethanol concentration reaches 80%. As this is the first manuscript addressing this interaction, some observations are speculative and require further investigation.

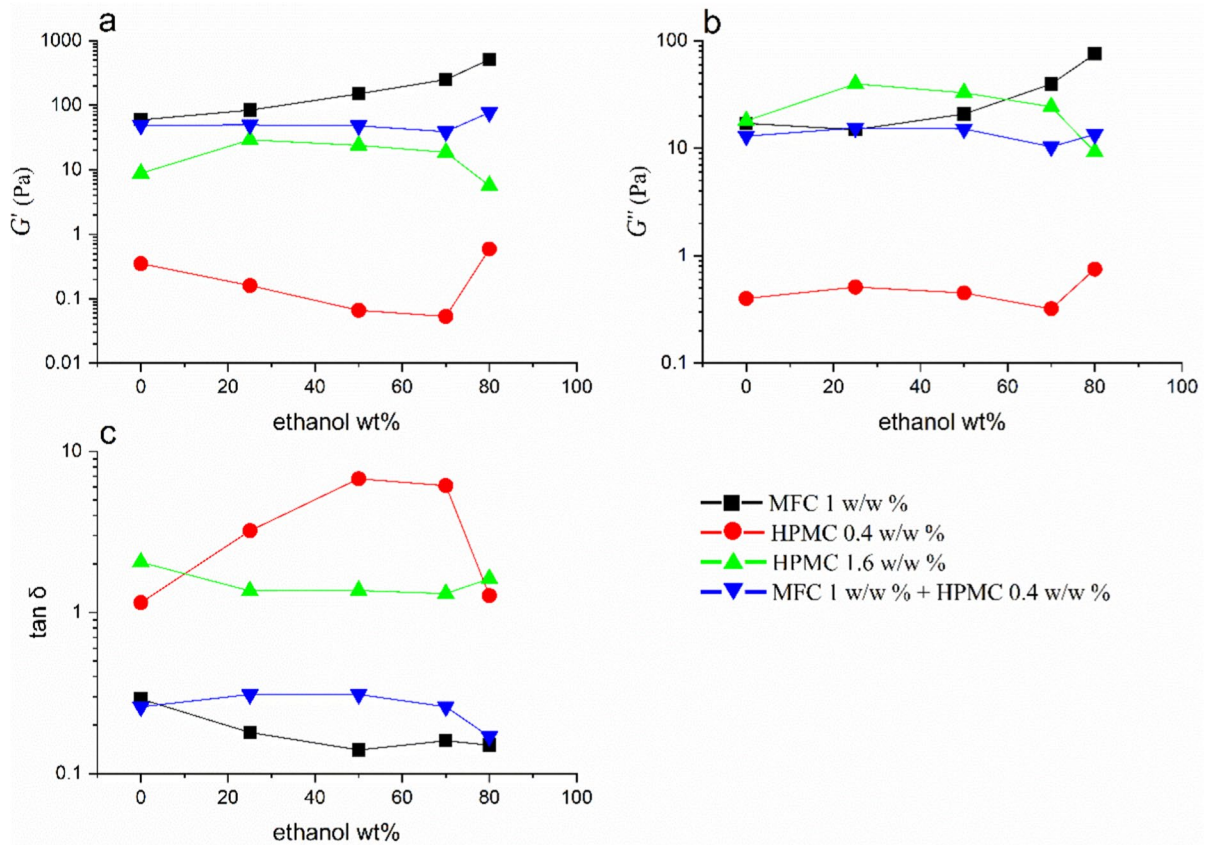


Fig. 3 Oscillatory frequency sweep, performed in a linear viscoelastic range at constant temperature 25 °C. MFC 1 w/w%: black square. HPMC 0.4 w/w%: red circle. HPMC 1.6 w/w%: green up triangle. MFC 1 w/w%+HPMC 0.4 w/w%: blue down triangle. **a** and **b** Storage modulus (G') and loss modulus

(G'') at 1 Hz for MFC, HPMC and MFC+HPMC dispersions in different ethanol concentrations, respectively; **c** $\tan \delta$ at 1 Hz for MFC, HPMC and MFC+HPMC dispersions in different ethanol concentrations

Flow sweep

Fig. SI-2 presents flow sweeps for MFC, HPMC, and MFC+HPMC dispersions at various ethanol and polymer concentrations. In Fig. SI-2b, flow sweeps for MFC at different polymer concentrations are depicted. The behavior of MFC appears to be non-Newtonian, exhibiting a decrease in apparent viscosity with increasing shear rate, indicative of shear-thinning behavior, consistent with prior findings using water as solvent (Agoda-Tandjawa et al. 2010; Iotti et al. 2011; Pääkko et al. 2007).

In water-based MFC dispersions, various concentrations exhibit a distinctive viscosity profile characterized by two regions of shear thinning, separated by a semi-plateau where viscosity remains relatively

stable. This intermediate viscosity state, noted in the literature for MFC/NFC systems, often manifests as a plateau (Agoda-Tandjawa et al. 2010; Jaiswal et al. 2021; Sorvari et al. 2014; Chen et al. 2002). Agoda-Tandjawa et al. (2010) and Chen et al. (2002) propose that during this phase, certain structural arrangements, possibly comprising individual fibers, emerge within the suspensions, causing a non-uniform flow pattern. This observation sheds light on the intricate rheological behavior of MFC dispersions, hinting at underlying structural transformations influencing their flow properties.

The viscosity dependence on shear rate is presented in Figs. 4a and SI-2a for various ethanol concentrations. Table SI-1 presents flow curve regression parameters using a Hershel-Buckley model. Notably,

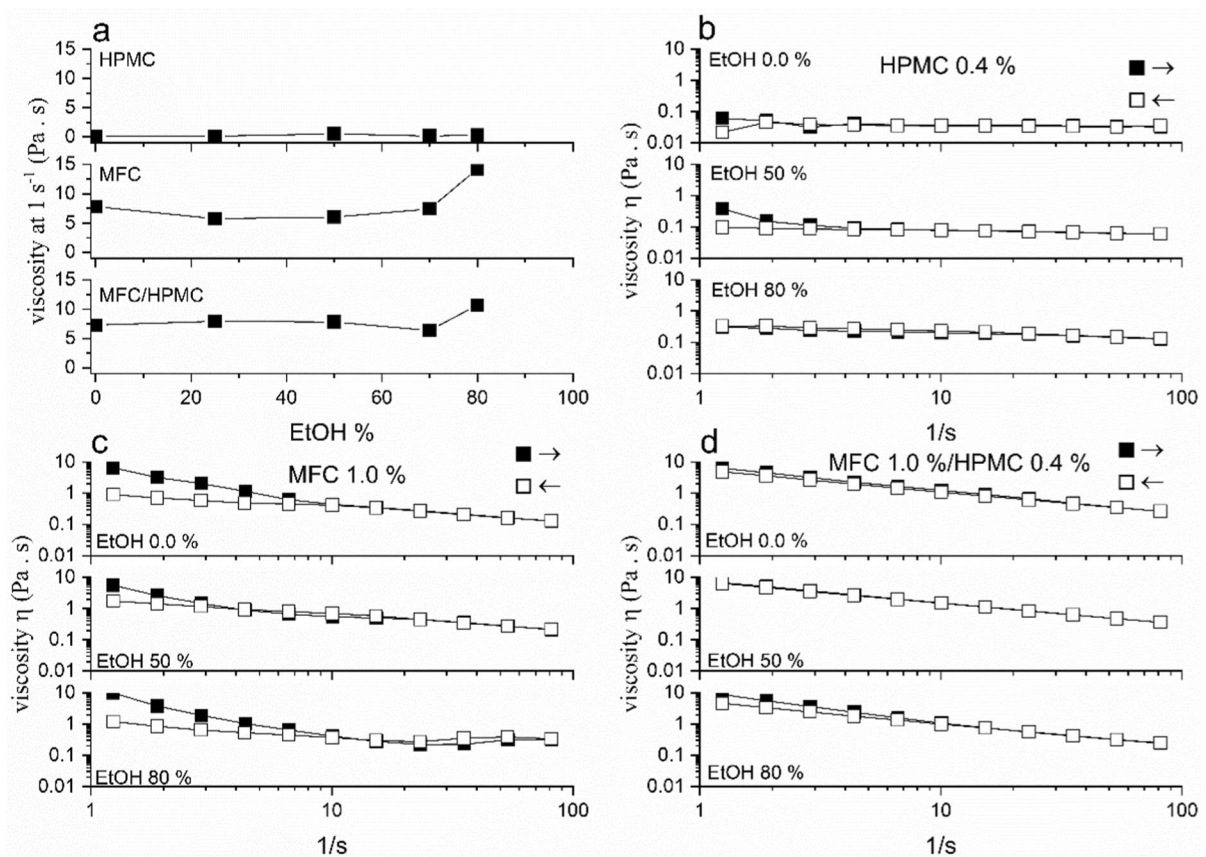


Fig. 4 Flow curves of polymers-ethanol/water mixtures. Increasing shear rates: solid symbols. Decreasing shear rates: open symbols. **a** Effect of ethanol on viscosity at 1 s^{-1} for HPMC, MFC and MFC+HPMC dispersions in different ethanol concentration. **b** Flow curve for 0.4 w/w% HPMC disper-

sions in different ethanol concentrations. **c** Flow curve for 1 w/w% MFC dispersions in different ethanol concentrations. **d** Flow curve for 1 w/w% MFC and 0.4 w/w% HPMC dispersions in different ethanol concentrations

MFC dispersions exhibit shear-thinning behavior, with an $n < 1$ (where n is the flow behavior index, $n < 1$ denotes shear-thinning fluids, $n = 1$ for Newtonian fluids, and $n > 1$ for shear-thickening fluids) (Ciftci et al. 2020), except for the suspension with 80% ethanol, which had an n of 1.99. In this case, the high ethanol concentration likely promotes greater fiber–fiber frictional contact.

Flow sweeps of HPMC dispersions at different polymer concentrations are shown in Fig. SI-2d. At all concentrations, HPMC dispersions exhibit shear-thinning behavior. However, at 0.4% HPMC, the n value of the dispersions, except for the sample with 80% ethanol, exceeds 0.8, indicating dilute and Newtonian solution behavior (Lue and Zhang 2009). Fig. SI-2c and SI-2d depict flow sweeps for HPMC

dispersions at various ethanol concentrations and polymer concentrations, respectively. At low HPMC concentrations (0.4%) (Fig. 4a), ethanol content does not seem to affect viscosity, likely due to the low polymer concentration. However, at higher polymer concentrations, ethanol initially increases viscosity up to a certain concentration, after which it appears to have no effect. This aligns with findings reported by Perinelli et al. (2021).

Fig. SI-2f shows flow sweeps for MFC+HPMC at different polymer concentrations, with flow curve regression parameters presented in Table SI-1. MFC+HPMC dispersions exhibit shear-thinning behavior like MFC and HPMC dispersions, albeit without a plateau region observed in MFC dispersions. Notably, yield stress is observed regardless of

ethanol concentration for MFC + HPMC dispersions, which does not occur for other dispersions except for MFC dispersions with ethanol concentrations above 80%. This effect likely arises from HPMC adsorption on MFC fibrils, decreasing the zeta potential to close to zero and increasing attraction between particles, leading to aggregation and increased viscosity and yield stress, similar to observed by Mosse et al. (2012).

To evaluate dispersion hysteresis, ascending and descending flow curves were conducted from 1 to 100 1/s and from 100 to 1 1/s (Fig. 4) under steady-state conditions. Table SI-1 shows hysteresis loop area obtained for HPMC, MFC, and MFC + HPMC samples. MFC dispersion at 0.0% ethanol exhibits a hysteresis loop at low shear rates. At 50% ethanol, positive hysteresis areas are observed at low and high shear rates, and negative hysteresis at medium shear rates, while at 80% ethanol, positive and negative areas occur at low and high shear rates, respectively. Hysteresis has been observed for various types of MFC dispersions (Agoda-Tandjawa et al. 2010; Blok et al. 2021; Martoia et al. 2015; Schenker et al. 2018, 2019). This time-dependent viscosity effect is attributed to changes in MFC dispersion structure under shear flow. In the absence of shear, MFC fibrils are randomly oriented, but under shear, they orient and align, reducing the viscosity.

Temperature ramp

Temperature ramps were conducted to assess the stability of MFC (Fig. 5a–b), HPMC (Fig. 5c–d), and MFC + HPMC (Fig. 5e–f) dispersions at varying ethanol concentrations. Three ascending ramps from 5 °C to 50 °C and three descending ramps from 50 °C to 5 °C were executed, with a heating and cooling rate of 10 °C/min, using a solvent trap.

All MFC dispersions exhibited $G' > G''$. At 0.0% ethanol, the MFC dispersion displayed pronounced instability, with a significant decrease in both moduli and non-coinciding forward and backward ramps. Conversely, MFC dispersions in ethanol exhibited a gradual decline in both moduli with well-overlapping ramps. Similar results were reported by Jia et al. (2014) for amorphous cellulose suspensions in water, attributing this behaviour to the weakening or disruption of intermolecular hydrogen bonds with increasing temperature. Regarding dispersions with ethanol,

it's plausible that ethanol, acting as a chaotropic agent, has already disrupted a significant portion of hydrogen bonds, thereby minimizing the temperature's impact.

In Fig. 5c–d, the temperature ramps for the HPMC dispersions reveal a typical pattern, with G' surpassing G'' and both moduli diminishing as temperature rises (Silva et al. 2008). The temperature ramps do not overlap, likely due to the low polymer concentration, as better overlap is observed at higher concentrations (results not depicted). Additionally, it's worth noting that the behavior remains quite similar for dispersions with ethanol, suggesting that ethanol has a minimal effect on intermolecular hydrogen bonds for HPMC in the range of concentrations evaluated.

Temperature ramps for MFC + HPMC dispersions are depicted in Fig. 5e–f. All dispersions exhibit a consistent pattern, with G' surpassing G'' and a gradual decline in moduli with increasing temperature. G' was around 100 Pa, with good overlap of the round-trip ramps. Firstly, this suggests that HPMC in ethanol smoothes the slope of the moduli versus temperature cycle and promotes overlapping of the round-trip ramps, indicating reduced intermolecular interaction due to hydrogen bonds with adsorbed HPMC on the fibrils. Secondly, ethanol appears to have no discernible effect in the presence of HPMC, mirroring observations in HPMC dispersions. Thus, it can be inferred that HPMC positively influences the stability of MFC dispersions.

Effect of urea

To evaluate polymer–polymer and polymer–solvent interactions, MFC and MFC + HPMC samples were prepared with 6 M urea, a well-known chaotropic agent effective in disrupting hydrogen bonds (Kjønksen et al. 2003; Kokufuta et al. 1998), which may also weaken hydrophobic interactions (Kokufuta et al. 1998).

Fig. SI-3 illustrates ascending and descending flow curves of MFC and MFC + HPMC dispersions with and without urea. Figs. SI-3a and SI-3b depict MFC flow curves with and without urea. MFC dispersions at 0.0% ethanol (Fig. SI-3a) with urea exhibited lower viscosity at low shear rates compared to MFC dispersions without urea, consistent with prior research (Jaishankar et al. 2015; Kjønksen et al. 2005), suggesting that a portion of the viscosity arises from

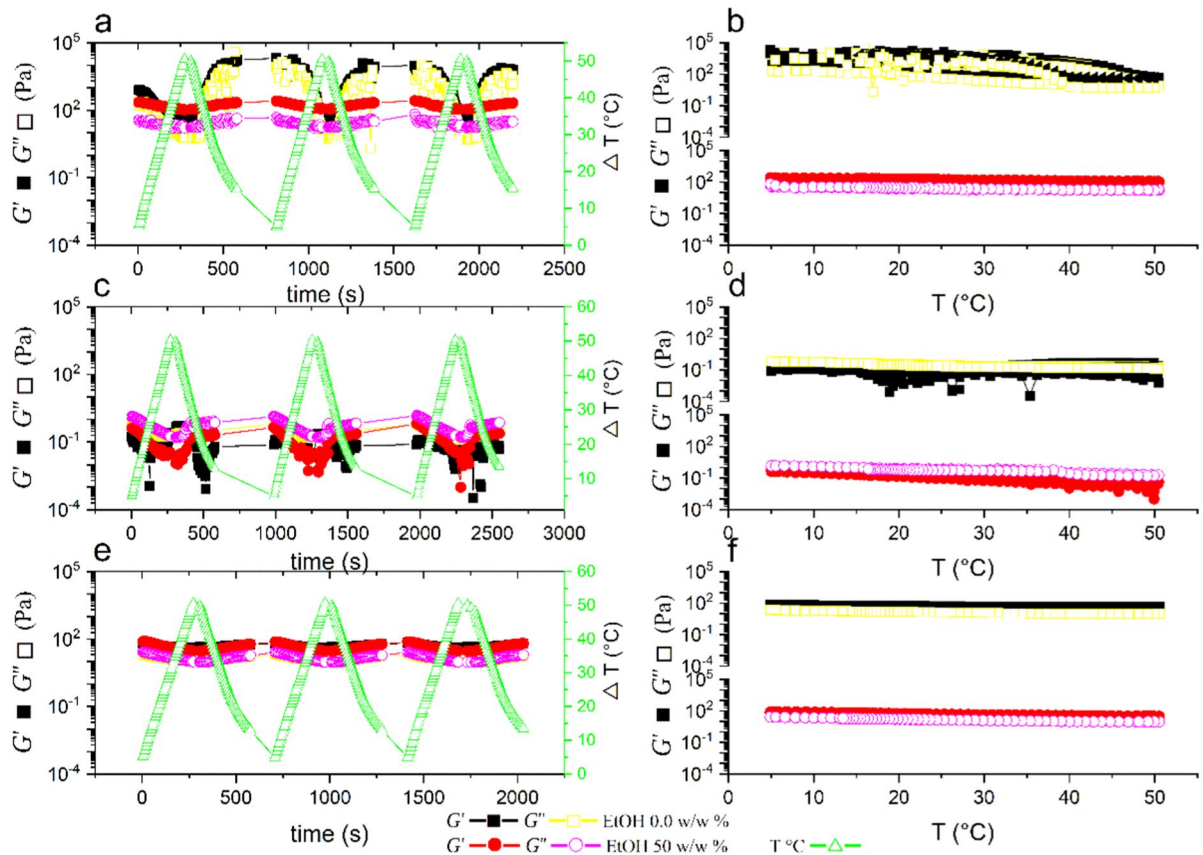


Fig. 5 Temperature sweep for MFC, HPMC and MFC+HPMC dispersions in 0.0 w/w% (G' – black solid square, G'' – yellow open square) and 50 w/w% (G' – red solid circle, G'' – magenta open circle) ethanol. **a** and **b** Storage modulus and loss modulus, as a function of temperature, for

1 w/w% MFC dispersions. **c** and **d** Storage modulus and loss modulus, as a function of temperature, for 0.4 w/w% HPMC dispersions. **e** and **f** Storage modulus and loss modulus, as a function of temperature, for 1.0 w/w% + 0.4 w/w% HPMC dispersions

hydrogen bonds. It's plausible, hypothetically, that urea's presence encourages fibril floc formation, leading to increased flow resistance at high shear rates. Moreover, MFC dispersion with urea demonstrated higher viscosity throughout the shear rate range during the back flow sweep, suggesting that urea facilitates better reassociation post-structure breakdown induced by shear.

MFC dispersions in ethanol/water (Fig. SI-3b) exhibited lower viscosity compared to MFC dispersions in water. Interestingly, the profiles of MFC dispersions with and without urea were similar in ethanol/water, with slightly lower viscosity at low shear rates in the presence of urea. Additionally, in both cases, the return sweep closely mirrored the initial sweep, indicating higher viscosity than MFC

dispersions without ethanol. This behavior could be attributed to ethanol acting as a chaotropic agent similar to urea, aligning with existing literature (Morel et al. 2020; Vorontsova et al. 2015).

Fig. SI-3c and SI-3d display MFC+HPMC flow sweeps with and without ethanol, respectively, and with and without urea. Like MFC dispersions, MFC+HPMC dispersions exhibited reduced hysteresis areas in both the presence of ethanol and urea, likely due to the chaotropic nature of urea and ethanol, disrupting hydrogen bonds. However, unlike MFC dispersions, MFC+HPMC dispersions with urea displayed higher viscosity. This could stem from a conformational change in the HPMC molecules adsorbed on the MFC, with urea potentially disrupting intra-molecular hydrogen bonds, leading to

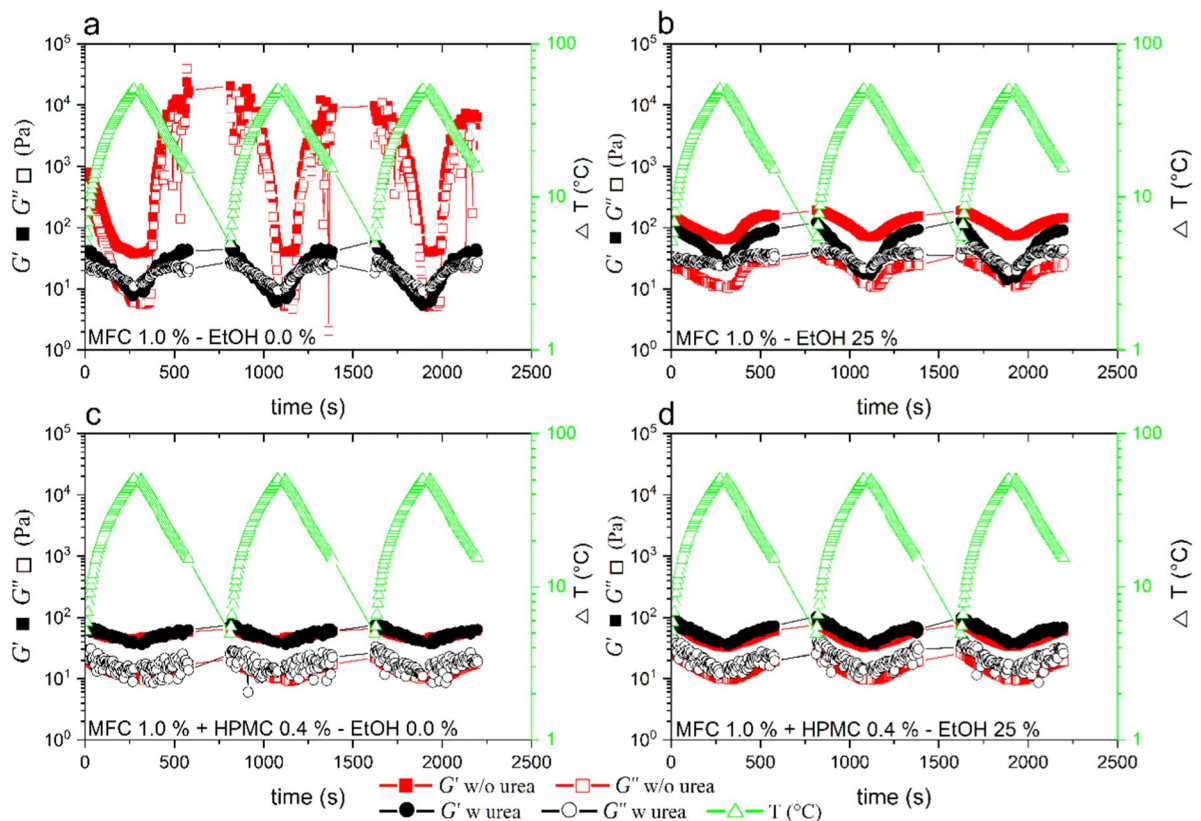


Fig. 6 Temperature sweep of polymers-ethanol/water mixtures with and without urea. Storage modulus with (black solid circles) and without urea (red solid square). Loss modulus with (black open circles). **a** Effect of urea on thermal behavior for MFC+HPMC dispersions at ethanol 0.0%. **b** Effect of urea

on thermal behavior for MFC+HPMC dispersions at ethanol 25%. **c** Effect of urea on thermal behavior for MFC dispersions at ethanol 0.0%. **d** Effect of urea on thermal behavior for MFC dispersions at ethanol 25%

extended chain conformations and increased viscosity in certain polymers, a phenomenon observed in chitosan, fenugreek gum, and xyloglucan (Tsaih and Chen 1997; Winkworth-Smith et al. 2016).

Figure 6 showcases temperature sweeps of MFC and MFC+HPMC dispersions with and without urea. MFC dispersions at 0.0 w/w% ethanol (Fig. 6a) exhibited unstable behavior, while those at 25% ethanol (Fig. 6b) displayed only a downturn in both moduli, indicating stability. With the addition of 6 M urea, both moduli decreased, sharply dropping to 0.0 w/w% dispersions. Additionally, the crossover between G' and G'' occurred at 25–35 °C and 31–48 °C for dispersions with and without ethanol, respectively. Notably, a more substantial decrease in moduli was observed for MFC dispersions without ethanol, possibly due to ethanol

acting as a chaotropic agent, disrupting a significant portion of intermolecular hydrogen bonds, leaving fewer for urea to disrupt. The crossing point of moduli G' and G'' suggests that hydrogen bonding and hydrophobic interactions are crucial for gel network formation and stability, a common observation in the presence of chaotropic agents (Sun and Arntfield 2012; Yan et al. 2021).

Figure 6c (0.0% ethanol) and 6d (25% ethanol) illustrate temperature ramps for MFC+HPMC dispersions with and without urea. In both cases, urea had no impact on both moduli, with good overlap compared to temperature sweeps for dispersions without urea. This indicates an interaction between MFC and HPMC and suggests that, in this case, intermolecular hydrogen bonds do not play a significant role in the gel network.

Table 1 Zeta potential for MFC, HPMC and MFC + HPMC in different ethanol concentrations

Polymer	Ethanol (% w/w)				
	0	25	50	70	80
MFC	-50.4 ± 1.6 mV	-28.0 ± 1.0 mV	-12.2 ± 1.0 mV	-6.2 ± 0.2 mV	-7.1 ± 0.1 mV
MFC + HPMC	-6.1 ± 0.2 mV	-4.4 ± 0.2 mV	-3.6 ± 0.2 mV	-6.0 ± 0.4 mV	-4.0 ± 0.2 mV
HPMC	0.0 ± 0.0 mV	-1.1 ± 0.5 mV	-2.0 ± 0.1 mV	-1.8 ± 0.1 mV	-1.6 ± 0.0 mV

Zeta potential

The impact of HPMC and ethanol concentration on the surface electrical charge of MFC was assessed by measuring the zeta potential (Table 1). At 0.0% ethanol, MFC dispersions exhibited a zeta potential of approximately -50 mV. With increasing ethanol concentration, there was a consistent decline in the zeta potential, reaching -6.2 – -7.1 mV. This decline is attributed to ethanol/water interactions and the lower dielectric constant of ethanol (24.5) compared to water (78.1) (Gözcü et al. 2023).

Conversely, in MFC + HPMC dispersions, the zeta potential remained stable within the range of ~ -4.0 to 6.1 mV, indicating no significant variation compared to pure MFC. This suggests minimal influence of ethanol on the zeta potential of MFC/HPMC dispersion. Moreover, the notable decrease in zeta potential suggests HPMC adsorption onto the MFC surface, resulting in increased distance between fibrils and the shear plane (Duro et al. 1998). No significant change in the zeta potential of MFC was observed with varying ethanol concentration.

Conclusions

The study aimed to investigate the thickening properties and rheological stability of MFC and MFC + HPMC dispersions in ethanol/water mixtures. Both ethanol addition and HPMC incorporation led to enhancements in rheological properties. Through concentration variation, phase diagrams were established, revealing phase separation, and distinguishing between liquid-like and gel-like behaviors via oscillatory rheometric measurements. Results highlighted the gel-like behavior of MFC and MFC + HPMC, primarily dictated by polymer concentrations with minor influence from ethanol. Ethanol significantly impacted the rheological characteristics, attributed

to its chaotropic nature, affecting network strength, thixotropic behavior, and stability. HPMC, by adsorbing onto MFC fibrils, induced system aggregation, influencing viscosity, thixotropy, and stability. Testing with urea, a potent chaotropic agent, provided insights into the governing interactions.

Acknowledgements The authors would like to thank Embrapa Forestry, Electronic Microscopy Center (CME/UFPR), BioPol (UFPR), and Federal University of Paraná (UFPR) for supporting this work.

Author Contribution Egon Petersohn Junior: Conceptualization, Methodology, Formal Analysis, Writing – Original Draft. Angelo Cezar Lucizani: Formal Analysis. Victor Veríssimo: Formal Analysis. Cassiano Pires: Methodology, Investigation. Alan Sulato de Andrade: Methodology, Investigation. Mailson de Matos: Methodology. Gisele Perissutti: Conceptualization. Washington Luiz Esteves Magalhaes: Conceptualization, Methodology, Funding acquisition, Supervision, Writing – Review. Rilton Alves de Freitas: Conceptualization, Methodology, Supervision, Writing – Review & Editing.

Funding This study was financed in part by the Coordenação de Aperfeiçoamento de Pessoal de Nível Superior—Brasil (CAPES)—Finance Code (Grant No. 001), Conselho Nacional de Desenvolvimento Científico e Tecnológico, (Grant No. 304446/2022-0), Financiadora de Estudos e Projetos, (Grant No. 0463/20)

Data Availability No datasets were generated or analysed during the current study.

Declarations

Competing interests The authors declare no competing interests.

References

Adeyeye MC, Jain AC, Ghorab MKM, Reilly Jr WJ (2002) Viscoelastic evaluation of topical creams containing microcrystalline cellulose/sodium carboxymethyl cellulose as

- stabilizer. *AAPS PharmSciTech* 3:16–25. <https://doi.org/10.1208/pt030208>
- Agoda-Tandjawa G, Durand S, Berot S, Blassel C, Gaillard C, Garnier C, Doublier JL (2010) Rheological characterization of microfibrillated cellulose suspensions after freezing. *Carbohydr Polym* 80:677–686. <https://doi.org/10.1016/j.carbpol.2009.11.045>
- Baby DK (2019) Rheology of hydrogels. In: Thomas S, Sarathchandran C, Chandran N (eds) *Rheology of polymer blends and nanocomposites theory, modelling and applications*. Elsevier, Amsterdam
- Bilbao-Sáinz C, Avena-Bustillos RJ, Wood DF, Williams TG, Mchugh TH (2010) Composite edible films based on hydroxypropyl methylcellulose reinforced with microcrystalline cellulose nanoparticles. *J Agric Food Chem* 58:3753–3760. <https://doi.org/10.1021/jf9033128>
- Blok AE, Bolhuis DP, Kibbelaar HVM, Bonn D, Velikov KP, Stieger M (2021) Comparing rheological, tribological and sensory properties of microfibrillated cellulose dispersions and xanthan gum solutions. *Food Hydrocoll* 121:107052. <https://doi.org/10.1016/j.foodhyd.2021.107052>
- Burdock GA (2007) Safety assessment of hydroxypropyl methylcellulose as a food ingredient. *Food Chem Toxicol* 45:2341–2351. <https://doi.org/10.1016/j.fct.2007.07.011>
- Butchosa N, Zhou Qi (2014) Water redispersible cellulose nanofibrils adsorbed with carboxymethyl cellulose. *Cellulose* 21:4349–4358. <https://doi.org/10.1007/s10570-014-0452-7>
- Cassanelli M, Norton I, Mills T (2017) Effect of alcohols on gellan gum gel structure: bridging the molecular level and the three-dimensional network. *Food Struct* 14:112–120. <https://doi.org/10.1016/j.foosr.2017.09.002>
- Chen B, Tatsumi D, Matsumoto T (2002) Floc structure and flow properties of pulp fiber suspensions. *J Soc Rheol Japan* 30:10–25
- Ciftci C, Goksu PA, Larsson AV, Riazanova HH, Øvrebø LW, Berglund LA (2020) Tailoring of rheological properties and structural polydispersity effects in microfibrillated cellulose suspensions. *Cellulose* 27:9227–9241. <https://doi.org/10.1007/s10570-020-03438-6>
- Costa VLD, Costa AP, Simões RMS (2019) Nanofibrillated cellulose rheology: effects of morphology, ethanol/acetone addition, and high NaCl concentration. *BioResources* 14:7636–7654. <https://doi.org/10.15376/biores.14.4.7636-7654>
- Dixit S, Crain J, Poon WCK, Finney JL, Soper AK (2002) Molecular segregation observed in a concentrated alcohol-water solution. *Nature* 416:829–832. <https://doi.org/10.1038/416829a>
- Duro R, Alvarez C, Martínez-Pacheco R, Gómez-Amoza JL, Concheiro A, Souto C (1998) The adsorption of cellulose ethers in aqueous suspensions of pyrantel pamoate: effects on zeta potential and stability. *Eur J Pharm Biopharm* 45:181–188. [https://doi.org/10.1016/S0939-6411\(97\)00103-3](https://doi.org/10.1016/S0939-6411(97)00103-3)
- Echeverria C, Fernandes SN, Almeida PL, Godinho MH (2016) Effect of cellulose nanocrystals in a cellulosic liquid crystal behaviour under low shear (regime I): structure and molecular dynamics. *Eur Polym J* 84:675–684. <https://doi.org/10.1016/j.eurpolymj.2016.10.009>
- Gold NA, Mirza TM, Avva U (2023) Alcohol sanitizer. In: *StatPearls* [Internet]. Treasure Island (FL): StatPearls Publishing. <https://www.ncbi.nlm.nih.gov/books/NBK513254/> Accessed 26 September 2023
- Gourlay K, van der Zwan T, Shourav M, Saddler J (2018) The potential of endoglucanases to rapidly and specifically enhance the rheological properties of micro/nanofibrillated cellulose. *Cellulose* 25:977–986. <https://doi.org/10.1007/s10570-017-1637-7>
- Gözcü O, Utkucan Kayacı H, Dou Y, Zhang W, Hedin N, Jasso-Salcedo AB, Kaiser A, Aygün SÇ (2023) Colloidal stabilization of submicron-sized zeolite NaA in ethanol-water mixtures for nanostructuring into thin films and nanofibers. *Langmuir* 39:192–203. <https://doi.org/10.1021/acs.langmuir.2c02241>
- Hubbe MA, Tayeb P, Joyce M, Tyagi P, Kehoe M, Dimic-Misic K, Pal L (2017) Rheology of nanocellulose-rich aqueous suspensions: a review. *BioResources* 12:9556–9661. <https://doi.org/10.15376/biores.12.4.Hubbe>
- Iotti M, Gregersen ØW, Moe S, Lenes M (2011) Rheological studies of microfibrillar cellulose water dispersions. *J Polym Environ* 19:137–145. <https://doi.org/10.1007/s10924-010-0248-2>
- IUPAC Compendium of Chemical Terminology, 3rd ed. International Union of Pure and Applied Chemistry; 2006. Online version 3.0.1, 2019. <https://doi.org/10.1351/goldbook.G02600>
- Jaishankar A, Wee M, Matia-Merino L, Goh KKT, McKinley GH (2015) Probing hydrogen bond interactions in a shear thickening polysaccharide using nonlinear shear and extensional rheology. *Carbohydr Polym* 123:136–145. <https://doi.org/10.1016/j.carbpol.2015.01.006>
- Jaiswal AK, Kumar V, Khakalo A, Lahtinen P, Solin K, Pere J, Toivakka M (2021) Rheological behavior of high consistency enzymatically fibrillated cellulose suspensions. *Cellulose* 28:2087–2104. <https://doi.org/10.1007/s10570-021-03688-y>
- Jia X, Chen Y, Shi C, Ye Y, Abid M, Jabbar S, Wang P, Zeng X, Tao Wu (2014) Rheological properties of an amorphous cellulose suspension. *Food Hydrocoll* 39:27–33. <https://doi.org/10.1016/j.foodhyd.2013.12.026>
- Jia X, Ranran Xu, Shen W, Xie M, Abid M, Jabbar S, Wang P, Zeng X, Tao Wu (2015) Stabilizing oil-in-water emulsion with amorphous cellulose. *Food Hydrocoll* 43:275–282. <https://doi.org/10.1016/j.foodhyd.2014.05.024>
- Jian Y, Handschuh-Wang S, Zhang J, Wei Lu, Zhou X, Chen T (2021) Biomimetic anti-freezing polymeric hydrogels: keeping soft-wet materials active in cold environments. *Mater Horiz* 8:351–369. <https://doi.org/10.1039/D0MH01029D>
- Joye II, McClements DJ (2013) Production of nanoparticles by anti-solvent precipitation for use in food systems. *Trends Food Sci Technol* 34:109–123. <https://doi.org/10.1016/j.tifs.2013.10.002>
- Kjøniksen AL, Hiorth M, Roots J, Nyström Bo (2003) Shear-induced association and gelation of aqueous solutions of pectin. *J Phys Chem B* 107:6324–6328. <https://doi.org/10.1021/jp0302358>
- Kjøniksen AL, Hiorth M, Nyström Bo (2005) Association under shear flow in aqueous solutions of pectin. *Eur*

- Polym J 41:761–770. <https://doi.org/10.1016/j.eurpolymj.2004.11.006>
- Klemm D, Kramer F, Moritz S, Lindström T, Ankerfors M, Gray D, Dorris A (2011) Nanocelluloses: a new family of nature-based materials. *Angew Chem Int Ed* 50:5438–5466. <https://doi.org/10.1002/anie.201001273>
- Kokol V (2022) Influence of hydroxyethyl and carboxymethyl celluloses on the rheology, water retention and surface tension of water-suspended microfibrillated cellulose. *Cellulose* 29:7063–7081. <https://doi.org/10.1007/s10570-022-04737-w>
- Kokufuta E, Suzuki H, Yoshida R, Yamada K, Hirata M, Kaneko F (1998) Role of hydrogen bonding and hydrophobic interaction in the volume collapse of a poly(ethylenimine) gel. *Langmuir* 14:788–795. <https://doi.org/10.1021/la9709103>
- Lameirinhas NS, Teixeira MC, Carvalho JPF, Valente BFA, Pinto RJB, Oliveira H, Luís JL, Pires L, Oliveira JM, Vilela C, Freire CSR (2023) Nanofibrillated cellulose/gellan gum hydrogel-based bioinks for 3D bioprinting of skin cells. *Int J Biol Macromol* 229:849–860. <https://doi.org/10.1016/j.ijbiomac.2022.12.227>
- Lue A, Zhang L (2009) Rheological behaviors in the regimes from dilute to concentrated in cellulose solutions dissolved at low temperature. *Macromol Biosci* 9:488–496. <https://doi.org/10.1002/mabi.200800231>
- Martoia F, Perge C, Dumont PJJ, Orgéas L, Fardin MA, Manneville S, Belgacem MN (2015) Heterogeneous flow kinematics of cellulose nanofibril suspensions under shear. *Soft Matter* 11:4742–4755. <https://doi.org/10.1039/C5SM00530B>
- Mašková E, Kubová K, Raimi-Abraham BT, Vllasaliu D, Vohlidalová E, Turánek J, Mašek J (2020) Hypromellose – a traditional pharmaceutical excipient with modern applications in oral and oromucosal drug delivery. *J Control Release* 324:695–727. <https://doi.org/10.1016/j.jconrel.2020.05.045>
- Medronho B, Romano A, Miguel MG, Stigsson L, Lindman B (2012) Rationalizing cellulose (in)solubility: reviewing basic physicochemical aspects and role of hydrophobic interactions. *Cellulose* 19:581–587. <https://doi.org/10.1007/s10570-011-9644-6>
- Morel MH, Pincemaille J, Chauveau E, Louhichi A, Violleau F, Menut P, Ramos L, Banc A (2020) Insight into gluten structure in a mild chaotropic solvent by asymmetrical flow field-flow fractionation (AsFIFFF) and evidence of non-covalent assemblies between glutenin and ω -gliadin. *Food Hydrocoll* 103:105676. <https://doi.org/10.1016/j.foodhyd.2020.105676>
- Mosse WKJ, Boger DV, Simon GP, Garnier G (2012) Effect of cationic polyacrylamides on the interactions between cellulose fibers. *Langmuir* 28:3641–3649. <https://doi.org/10.1021/la2049579>
- Naeli MH, Milani JM, Farmani J, Zargaraan A (2020) Development of innovative ethyl cellulose-hydroxypropyl methylcellulose biopolymer oleogels as low saturation fat replacers: physical, rheological and microstructural characteristics. *Int J Biol Macromol* 156:792–804. <https://doi.org/10.1016/j.ijbiomac.2020.04.087>
- Nath PC, Debnath S, Sridhar K, Inbaraj BS, Nayak PK, Sharma M (2023) A comprehensive review of food hydrogels: principles, formation mechanisms, microstructure, and its applications. *Gels* 9(1):1. <https://doi.org/10.3390/gels9010001>
- Nechyporchuk O, Belgacem MN, Bras J (2016) Production of cellulose nanofibrils: a review of recent advances. *Ind Crops Prod* 93:2–25. <https://doi.org/10.1016/j.indcrop.2016.02.016>
- Onori G, Santucci A (1996) Dynamical and structural properties of water/alcohol mixtures. *J Mol Liq* 69:161–181. [https://doi.org/10.1016/S0167-7322\(96\)90012-4](https://doi.org/10.1016/S0167-7322(96)90012-4)
- Pääkko M, Ankerfors M, Kosonen H, Nykänen A, Ahola S, Österberg M, Ruokolainen J, Laine J, Larsson PT, Ikkala O, Lindström T (2007) Enzymatic hydrolysis combined with mechanical shearing and high-pressure homogenization for nanoscale cellulose fibrils and strong gels. *Biomacromol* 8:1934–1941. <https://doi.org/10.1021/bm061215p>
- Peng B, Tang J, Wang P, Luo J, Xiao P, Lin Y, Tam KC (2018) Rheological properties of cellulose nanocrystal-polymeric systems. *Cellulose* 25:3229–3240. <https://doi.org/10.1007/s10570-018-1775-6>
- Perinelli DR, Berardi A, Bisharat L, Cambriani A, Ganzetti R, Bonacucina G, Cespi M, Palmieri GF (2021) Rheological properties of cellulosic thickeners in hydro-alcoholic media: the science behind the formulation of hand sanitizer gels. *Int J Pharm* 604:120769. <https://doi.org/10.1016/j.ijpharm.2021.120769>
- Raj P, Mayahi A, Lahtinen P, Varanasi S, Garnier G, Martin D, Batchelor W (2016) Gel point as a measure of cellulose nanofibre quality and feedstock development with mechanical energy. *Cellulose* 23:3051–3064. <https://doi.org/10.1007/s1007/s10570-016-1039-2>
- Rathod HJ, Mehta DP (2015) A review on pharmaceutical gel. *Int J Pharm Sci* 1:33–47
- Rezayati Charani P, Dehghani-Firozabadi M, Afra E, Shakeri A (2013) Rheological characterization of high concentrated MFC gel from kenaf unbleached pulp. *Cellulose* 20:727–740. <https://doi.org/10.1007/s10570-013-9862-1>
- Schenker M, Schoelkopf J, Gane P, Mangin P (2018) Quantification of flow curve hysteresis data—a novel tool for characterising microfibrillated cellulose (MFC) suspensions. *Appl Rheol* 28(2):201822945. <https://doi.org/10.3933/applrheol-28-22945>
- Schenker M, Schoelkopf J, Gane P, Mangin P (2019) Rheology of microfibrillated cellulose (MFC) suspensions: influence of the degree of fibrillation and residual fibre content on flow and viscoelastic properties. *Cellulose* 26:845–860. <https://doi.org/10.1007/s10570-018-2117-4>
- Silva SMC, Pinto FV, Antunes FE, Miguel MG, Sousa JJS, Pais AACC (2008) Aggregation and gelation in hydroxypropylmethyl cellulose aqueous solutions. *J Colloid Interface Sci* 322:333–340. <https://doi.org/10.1016/j.jcis.2008.08.056>
- Silva Da, Marcelo A, Calabrese V, Schmitt J, Celebi D, Scott JL, Edler KJ (2018) Alcohol induced gelation of tempoxidized cellulose nanofibril dispersions. *Soft Matter* 14:9243–9249. <https://doi.org/10.1039/C8SM01815D>
- Sorvari A, Saarinen T, Haavisto S, Salmela J, Vuoriluoto M, Seppälä J (2014) Modifying the flocculation of microfibrillated cellulose suspensions by soluble polysaccharides under conditions unfavorable to adsorption. *Carbohydr*

- Polym 106:283–292. <https://doi.org/10.1016/j.carbpol.2014.02.032>
- Sun XD, Arntfield SD (2012) Molecular forces involved in heat-induced pea protein gelation: effects of various reagents on the rheological properties of salt-extracted pea protein gels. *Food Hydrocoll* 28:325–332. <https://doi.org/10.1016/j.foodhyd.2011.12.014>
- Tian Y, Song Q, Liu Z, Ye F, Zhou Y, Zhao G (2022) Linear and non-linear rheological properties of water-ethanol hybrid pectin gels for aroma enhancement. *Food Chem. X* 14:100328. <https://doi.org/10.1016/j.fochx.2022.100328>
- Tsaih ML, Chen RH (1997) Effect of molecular weight and urea on the conformation of chitosan molecules in dilute solutions. *Int J Biol Macromol* 20:233–240. [https://doi.org/10.1016/S0141-8130\(97\)01165-3](https://doi.org/10.1016/S0141-8130(97)01165-3)
- Tzoumaki MV, Moschakis T, Biliaderis CG (2013) Effect of soluble polysaccharides addition on rheological properties and microstructure of chitin nanocrystal aqueous dispersions. *Carbohydr Polym* 95:324–331. <https://doi.org/10.1016/j.carbpol.2013.02.066>
- Villa C, Russo E (2021) Hydrogels in hand sanitizers. *Materials* 14(7):1577. <https://doi.org/10.3390/ma14071577>
- Vorontsova MA, Chan HY, Lubchenko V, Vekilov PG (2015) Lack of dependence of the sizes of the mesoscopic protein clusters on electrostatics. *Biophys J* 109:1959–1968. <https://doi.org/10.1016/j.bpj.2015.09.025>
- Wakisaka A, Komatsu S, Usui Y (2001) Solute-solvent and solvent-solvent interactions evaluated through clusters isolated from solutions: preferential solvation in water-alcohol mixtures. *J Mol Liq* 90:175–184. [https://doi.org/10.1016/S0167-7322\(01\)00120-9](https://doi.org/10.1016/S0167-7322(01)00120-9)
- Wang Y, Long Yu, Xie F, Li S, Sun Q, Liu H, Chen L (2018) On the investigation of thermal/cooling-gel biphasic systems based on hydroxypropyl methylcellulose and hydroxypropyl starch. *Ind Crops Prod* 124:418–428. <https://doi.org/10.1016/j.indcrop.2018.08.010>
- Winkworth-Smith CG, Macnaughtan W, Foster TJ (2016) Polysaccharide structures and interactions in a lithium chloride/urea/water solvent. *Carbohydr Polym* 149:231–241. <https://doi.org/10.1016/j.carbpol.2016.04.102>
- Xu B (2009) Gels as functional nanomaterials for biology and medicine. *Langmuir* 25:8375–8377. <https://doi.org/10.1021/la900987r>
- Yan JN, Yi Nan Du, Jiang XY, Han JR, Pan JF, Hai Tao Wu (2021) Intermolecular interaction in the hybrid gel of scallop (*Patinopecten Yessoensis*) male gonad hydrolysates and κ -carrageenan. *J Food Sci* 86:792–802. <https://doi.org/10.1111/1750-3841.15618>
- Yuan Yi, Wang L, Ruo Jun Mu, Gong J, Wang Y, Li Y, Ma J, Pang J, Chunhua Wu (2018) Effects of konjac glucomannan on the structure, properties, and drug release characteristics of agarose hydrogels. *Carbohydr Polym* 190:196–203. <https://doi.org/10.1016/j.carbpol.2018.02.049>
- Zhang Y, Song Q, Tian Y, Zhao G, Zhou Y (2022) Insights into biomacromolecule-based algogels: a review on their synthesis. *Charact Appl. Food Hydrocoll* 128:107574. <https://doi.org/10.1016/j.foodhyd.2022.107574>
- Zhou Y, Liangliang W, Tian Y, Li R, Zhu C, Zhao G, Cheng Y (2020) A novel low-alkali konjac gel induced by ethanol to modulate sodium release. *Food Hydrocoll* 103:105653. <https://doi.org/10.1016/j.foodhyd.2020.105653>

Publisher's Note Springer Nature remains neutral with regard to jurisdictional claims in published maps and institutional affiliations.

Springer Nature or its licensor (e.g. a society or other partner) holds exclusive rights to this article under a publishing agreement with the author(s) or other rightsholder(s); author self-archiving of the accepted manuscript version of this article is solely governed by the terms of such publishing agreement and applicable law.